ФІЗИКА І ХІМІЯ ТВЕРДОГО ТІЛА
Т. 9, № 2 (2008) С. 312-318

PHYSICS AND CHEMISTRY OF SOLID STATE
V. 9, № 2 (2008) P. 312-318

PACS: 71.20.-B, 71.18.+Y

ISSN 1729-4428

G.P. Chuiko, D.M. Stepanchikov

Geometrical way of determination of effective masses and densities of states within generalized Kildal's model

Kherson National Technical University, Department of General and Applied Physics, Laboratory of Solid State Theory, Beryslawske Shosse, 24, 73008, Kherson, Ukraine, phone: +38(0552)326922, e-mail: step_75@mail.ru

A new geometrical approach to the calculation of effective masses of carriers as well as of densities of states within generalized Kildal's model presents itself. The computations were conducted for tetragonal phosphides of cadmium and zinc (Cd_3P_2, Zn_3P_2) both belonging to the spatial group $P4_2/nmc$ (D_{4h}^{15}). The transversal and the longitudinal effective masses directly associate with semi-axes of the equal energy surfaces. Authors evaluated also the effective masses of the density of states and the coefficients of anisotropy. It was shown that the geometrical approach allows the determining and the classifying the points of singularities with high reliability. The attained results showed that the conductivity bands for both materials are about isotropic, but valence bands are not. The density of states for the top of the heavy holes band has the non-zero limit as a specific feature.

Keywords: Kildal's model, effective masses, densities of states, anisotropy, $A_3^{II}B_2^{V}$ compounds.

Стаття поступила до редакції 28.04.2007; прийнята до друку 15.02.2008

Introduction

The knowledge about effective masses as well as densities of states is considered necessary for both predictions and interpretations of the wide complex of semiconductors physical properties. However, the finding of both above mentioned functions is frequently a hardly calculable problem. It is caused mainly by the complexity or/and even by the implicit declaration of dependencies of a carrier's energy versus a wave vector. For that reason the analytical expressions are often either unattainable or too bulky. Even the numerical calculations are sometimes too expensive as for the expenditures both of computer time and human efforts. Conversely, a „roundabout ways" bring success now and again, so an example of such „maneuver" became accordingly a subject of this paper.

Kildal's model [1] is widely used for the describing of a lot of the one-axis crystals, in particular for materials with common chemical formula $A_3^{II}B_2^{V}$. However, this model has been developed for pseudo-cube crystals with the symmetry center and not takes into account small tetragonal tensions, which are inherent for $A_3^{II}B_2^{V}$ crystals. That is why the somewhat more general, but also the more complicated, version of this model was offered in [2].

A new geometrical approach to the calculation of effective masses of carriers as well as of densities of states within model [2] is presented here. More exactly, it is truthful within simpler variant of [2] for the crystals with the symmetry center. A method of the determination of the special (Van Hove) points of functions of the density of states would here also present itself. The main idea of the approach is based on association of both necessary functions with the specific form of Surfaces of Equal Energies (named as SEE below) following from theory of [2].

Our computations were conducted for tetragonal phosphides of cadmium and zinc (Cd_3P_2, Zn_3P_2), belonging both to the spatial group $P4_2/nmc$ (D_{4h}^{15}). Such a choice was grounded on the perspective peculiarities of these crystals for optoelectronic purposes. Cadmium phosphide, for instance, is well-known material for infrared lasers [3] and thereto recently was described as an effective quantum amplifier for optical fiber-lines [4]. Zinc phosphide is acknowledged as a cheap material for high efficiency solar elements, having an excellent direct optical gap about 1.51 eV [5,6].

I. The method of calculations

The tensor of an inverse dynamical effective mass is classically [7] determined itself by some dispersion law $\varepsilon(\mathbf{k})$:

$$\frac{1}{m^*_{\alpha\beta}} = \frac{1}{\hbar^2}\frac{\partial^2\varepsilon}{\partial k_\alpha \partial k_\beta} \qquad (1)$$

where ε is carrier's energy; k_α is a component of the wave vector $\mathbf{k}$; $\alpha,\beta=(x,y,z)=(1,2,3)$ are coordinates indicators. This tensor is symmetrical as for a transposition of its indicators and might be reduced to its simplest form (i.e. to so-called form within main axes) in any extreme point $\mathbf{k_0}$. Let it be admitted that coordinate axes (x,y,z) are directed along the main axes of this tensor. In that case the dispersion law may be presented in the simple quadratic form [8] nearby to $\mathbf{k_0}$:

$$\varepsilon_n(\mathbf{k})-\varepsilon_n(\mathbf{k_0})=\sum_\alpha\frac{\hbar^2 q_\alpha^2}{2m_\alpha^*} \qquad (2)$$

where $n=1,2,...$ are energy bands numbers; $\mathbf{q}=\mathbf{k}-\mathbf{k_0}$; $m_\alpha^*=m_{\alpha\alpha}^*$.

A condition $\varepsilon_n(\mathbf{k})-\varepsilon_n(\mathbf{k_0})=const=\varepsilon$ corresponds to the surfaces of equal energies (SEE) of second order inside the wave vectors space. The expression (2) may be rewritten nearby to the extreme point as follows:

$$\frac{\hbar^2 q_x^2}{2m_x^*\varepsilon}+\frac{\hbar^2 q_y^2}{2m_y^*\varepsilon}+\frac{\hbar^2 q_z^2}{2m_z^*\varepsilon}=1 \qquad (3)$$

Therefore effective masses associate themselves with semi-axes of a surface of second order (3). This surface may be moderately close to the real SEE in the vicinity of the band extreme. Furthermore, if the real dispersion law can be expressed in the form (3) then such geometrical interpretation of effective masses would be proper even within wider interval of energies.

The dispersion law in framework of model [2] has such a form nearby the point **k** = 0 and with spherical coordinates (k,θ,φ):

$$(\Gamma(\varepsilon)-(\mathrm{Pk})^2(\mathrm{f_1}(\varepsilon)\sin^2\theta+\mathrm{f_2}(\varepsilon)\cos^2\theta))^2-(\mathrm{Pk})^2\mathrm{f_3^2}(\varepsilon)\sin^2\theta=0 \qquad (4)$$

Hamiltonian (4) describes a surface of rotation around the main crystalline axis. This Hamiltonian is of fourth order obviously what is for k [2].

On the other hand it might be simplified to the two identical surfaces, both of second order, under the additional condition: $f_3(\varepsilon)=0$. Physically this condition means the presence of the symmetry center into a crystal. Namely so and is for our materials.

Let us rewrite the simplified equation (4) with Cartesian coordinates and in accordance with the above supposition:

$$(k_x^2+k_y^2)P^2f_1(\varepsilon)+k_z^2P^2f_2(\varepsilon)-\Gamma(\varepsilon)=0 \qquad (5)$$

Certainly, the equation (5) describes a surface of second order. It can be rewritten in the form (3) as follows:

$$\frac{k_x^2+k_y^2}{s_x a^2}+\frac{k_z^2}{s_z b^2}=1 \qquad (6)$$

Here $s_\alpha=\pm1$ and it is a factor, which determines the sign of item; $a(\varepsilon)$ and $b(\varepsilon)$ are semi-axes of the surface. Both are connected with parameters of (5) as follows:

$$s_x a^2(\varepsilon)=\frac{\Gamma(\varepsilon)}{P^2 f_1(\varepsilon)};\quad s_z b^2(\varepsilon)=\frac{\Gamma(\varepsilon)}{P^2 f_2(\varepsilon)} \qquad (7)$$

Polynomials $\Gamma(\varepsilon),f_1(\varepsilon),f_2(\varepsilon)$ were described in [2]:

$$\Gamma(\varepsilon)=\varepsilon(\varepsilon-\varepsilon_g)\left[(\varepsilon+2\Delta/3)(\varepsilon+\delta+\Delta/3)-2\Delta^2/9\eta^2\right] \qquad (8)$$

$$f_1(\varepsilon)=(\varepsilon+\Delta/3)(\varepsilon+\delta+\Delta/3)-\Delta^2/9\eta^2 \qquad (9)$$

$$f_2(\varepsilon)=\eta^{-4}\varepsilon(\varepsilon+2\Delta/3) \qquad (10)$$

Thereto: (ε_g,Δ,P) – are three well-known Kane's parameters (the energy gap, the spin-splitting parameter and the matrix element of the impulse); δ - is the known parameter of the crystal field; η - is the scalar factor taking into account the deformation of the lattice [2].

Comparison of the equations (3) and (6,7) let's to get the expressions for the main components of the tensor of effective masses:

$$m_\perp^*=\frac{\hbar^2\Gamma(\varepsilon)}{2P^2\varepsilon f_1(\varepsilon)} \qquad (11)$$

$$m_\parallel^*=\frac{\hbar^2\Gamma(\varepsilon)}{2P^2\varepsilon f_2(\varepsilon)} \qquad (12)$$

Whereupon we can also evaluate the effective mass of the density of states as well as the coefficient of anisotropy:

$$m_d=\left|\sqrt[3]{m_\parallel^*(m_\perp^*)^2}\right|=\left|\frac{\hbar^2\Gamma(\varepsilon)}{2P^2\varepsilon\sqrt[3]{f_1(\varepsilon)^2 f_2(\varepsilon)}}\right| \qquad (13)$$

$$\xi(\varepsilon)=\left|\frac{m_\perp^*}{m_\parallel^*}\right|=\left|\frac{f_2(\varepsilon)}{f_1(\varepsilon)}\right| \qquad (14)$$

The surface integration on the SEE is usually used for the determination of the density of states inside an energy band [8]:

$$g(\varepsilon)\equiv\frac{dN}{d\varepsilon}=\frac{sV}{8\pi^3}\oint_{S_n(\varepsilon)}\frac{dS}{|grad_{\mathbf{k}}\varepsilon(\mathbf{k})|} \qquad (15)$$

Where s is the degeneration index ($s=2$ for crystals with the symmetry center); V is the crystal volume; $S_n(\varepsilon)$ - the SEE.

Nevertheless, there exists yet the Luttinger's theorem [9]. It connects the volume inside SEE $\tau(\varepsilon)$ with the quantity of states $N(\varepsilon)$ which contains itself inside energy interval $[\varepsilon_1,\varepsilon_2]$:

$$N(\varepsilon)=\frac{s\tau(\varepsilon)}{8\pi^3} \qquad (16)$$

The density of states is evidently the first derivative of $N(\varepsilon)$:

$$g(\varepsilon)=\frac{dN}{d\varepsilon}=\frac{s}{8\pi^3}\left|\frac{d\tau(\varepsilon)}{d\varepsilon}\right| \qquad (17)$$

All of our SEE are the surfaces of rotation of a curve of second order ($k_\perp^2/s_x a^2+k_z^2/s_z c^2=1$) around the polar axis k_z [10]. Its direction coincides with the main crystal axis. Therefore the internal volume of such SEE may be expressed as follows:

$$\tau=\int_{k_{z0}}^{k_{zm}} S(k_z)dk_z=\begin{cases}\frac{4}{3}\pi a^2(\varepsilon)b(\varepsilon);\\ 2\pi a^2(\varepsilon)k_{zm}\left(1+\frac{k_{zm}^2}{3b^2(\varepsilon)}\right);\\ 2\pi a^2(\varepsilon)\left(\frac{k_{zm}^3}{3b^2(\varepsilon)}-k_{zm}+\frac{2b(\varepsilon)}{3}\right);\end{cases} \qquad (18)$$

In formula (18) the equations are written for ellipsoid ($s_x=s_z=1$), hyperboloid of one sheet ($s_x=1;s_z=-1$) and hyperboloid of two sheets ($s_x=-1;s_z=1$) SEE respectively. The limits of integration (18) looks as

$$k_{z0}=\begin{cases}-b(\varepsilon); & (s_x=s_z=1)\\ -k_{zm}; & (s_x=1;s_z=-1)\\ b(\varepsilon); & (s_x=-1;s_z=1)\end{cases} \qquad (19)$$

$$k_{zm}=k(\varepsilon,\theta_m)\cos(\theta_m) \qquad (20)$$

where k_{zm} is the maximal projection of the wave vector $\mathbf{k}$ on the polar axis, whereas $k(\varepsilon,\theta_m)$ is the solution of (4) under condition $f_3(\varepsilon)=0$. The angle θ_m was determined in [11]:

$$\theta_m=\arccos\left(\sqrt{\frac{f_1(\varepsilon)-2\left(\frac{\pi}{a_0}\right)^2\Gamma(\varepsilon)}{f_1(\varepsilon)-f_2(\varepsilon)}}\right) \qquad (21)$$

where a_0 is the lattice parameter in the plane perpendicular to the main axis.

Now there is no problem to get the expressions for the densities of states using the equations (17-21) for same three distributions of sign factors like to expressions (18):

$$g(\varepsilon)=\begin{cases}\frac{a}{3\pi^2}\left|2b\frac{da}{d\varepsilon}+a\frac{db}{d\varepsilon}\right|\\ \frac{a}{2\pi^2}\left|2k_{zm}\left(1+\frac{k_{zm}^2}{3b^2}\right)\frac{da}{d\varepsilon}+\frac{a}{2}\left(2\frac{dk_{zm}}{d\varepsilon}\left(\frac{k_{zm}^2}{b^2}+1\right)-\frac{4k_{zm}^3}{3b^3}\frac{db}{d\varepsilon}\right)\right|\\ \frac{a}{\pi^2}\left|\left(\frac{2b}{3}-k_{zm}+\frac{k_{zm}^3}{3b^2}\right)\frac{da}{d\varepsilon}+\frac{a}{2}\left(\frac{2}{3}\frac{db}{d\varepsilon}\left(1-\frac{k_{zm}^3}{b^3}\right)+\frac{dk_{zm}}{d\varepsilon}\left(\frac{k_{zm}^2}{b^2}-1\right)\right)\right|\end{cases} \qquad (22)$$

Some singularities must be observable for the functions (22) at the points, where the velocity of carriers tends to zero: $\mathbf{v}=grad_{\mathbf{k}}\varepsilon(\mathbf{k})\to 0$. It follows from the integral (15) straight away. Such critical points might be of four types: minima (M_0), maxima (M_3), and two kinds of saddle points (M_1 and M_2). These singularities can be located not only at the center of the Brillouine zone but at other symmetrical points [8].

The geometrical approach allows the determining and the classifying of these singularities with the reliability. Let it be assumed that $\mathbf{k}_c$ is a critical point. Since the function $\varepsilon(\mathbf{k})$ might be extended in Taylor's series as a continuous function of its argument nearby $\mathbf{k}_c$:

$$\varepsilon_n(k)=\varepsilon_n(k_c)+\alpha_x(k_x-k_{c_x})^2+\alpha_y(k_y-k_{c_y})^2+\alpha_z(k_z-k_{c_z})^2+... \qquad (23)$$

The linear items were gone from (23) because $grad_{\mathbf{k}}\varepsilon(\mathbf{k})\big|_{\mathbf{k}=\mathbf{k}_c}=0$ for the critical point. It is a well idea to write the coefficients of series (23) across the effective masses. Although because those and these are straight associated with second derivatives of the function $\varepsilon(\mathbf{k})$ i.e. and between itself as well:

$$\alpha_x=\alpha_y=\frac{\hbar^2}{2m_\perp^*};\alpha_z=\frac{\hbar^2}{2m_{\|}^*} \qquad (24)$$

Thus the all analysis of type of a critical point is merely the tacking into consideration the set of effective masses signs: $\left(sign(m_\perp^*),sign(m_{II}^*)\right)$. Such simple rules are working here:

$$(+,+)\to M_0;\ (-,-)\to M_3;\quad (+,-)\to M_1;\ (-,+)\to M_2 \qquad (25)$$

The digital parameters used in our calculations are collected in the table 1.

Table 1.

Параметр	ε_g, eV	Δ, eV	P, eV·m	η	δ, eV	a_0, Å
Cd_3P_2	0,53 [3]	0,15 [6]	$7{,}2\cdot10^{-10}$ [12]	0,99090 [6]	0,02 [13]	8,7537 [14]
Zn_3P_2	1,51 [6]	0,11 [6]	$7{,}8\cdot10^{-10}$ [12]	0,99716 [6]	0,03 [13]	8,0889 [14]

Table 2.

		c-band	hh-band	lh-band	so-band
Cd_3P_2	ε_0, eV	0,53	0	-0,0138	-0,1591
	$m_\perp^* / m_0$	0,0424	-0,0783	-0,1679	-0,1690
	$m_\parallel^* / m_0$	0,0425	7,1753	-0,0655	-0,1192
	m_d / m_0	0,0425 (0,048 [11]) (0,0455 [15]) (0,0475 [18])	0,3531 (0,664 [11]) (0,373 [15]) (0,51 [19])	0,1227 (0,155 [11]) (0,068 [15]) (0,13 [18])	0,1504 (0,169 [11])
	ξ	0,9978	0,0109	2,5623	1,4176
Zn_3P_2	ε_0, eV	1,51	0	-0,0178	-0,1221
	$m_\perp^* / m_0$	0,0972	-0,1901	-0,4046	-0,3611
	$m_\parallel^* / m_0$	0,0979	24,1506	-0,1782	-0,2101
	m_d / m_0	0,0974 (0,2 [5]) (0,128 [16])	0,9554 (0,22 [5])	0,3079	0,3015
	ξ	0,9922	0,0078	2,2706	1,7187

II. Results of computations and their discussion

Dispersion equation (5) has four non-identical solutions describing the conductivity band, the heavy holes band, the light holes and spin-orbital split band respectively (see fig.1). The top of the hh-band is selected as the energy counting zero. Two of the three valence bands (hh and lh) have the limited width.

Ellipsoidal SEE describes the conductivity bands of both materials. Their coefficients of anisotropy just a bit differ from one (see table 2). Therefore both the transversal effective mass and the longitudinal effective mass are almost one and the same. The ellipsoid of SEE differs from a sphere just symbolically. Both materials demonstrate the linear energetic dependences (fig.2) for effective masses of electrons in addition to above pointed out. The exception is only narrow interval of energies

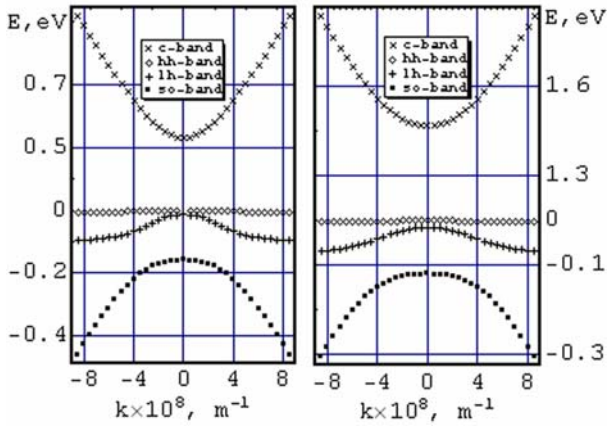

Fig. 1. Energy bands of Cd_3P_2 (a) and Zn_3P_2 (b) (for $\theta = \pi/4$).

adjoining to the bottom of the c-band.

The valence bands of the heavy and light holes at room temperatures are practically degenerated into the bargain to their mentioned limited width. Therefore it is possible to converse separately about effective masses for each of both bands just at very low temperatures, if to overcome the degeneration. It admits below as if that is true. There appears the nonlinear dependence of effective masses versus energy (fig. 3). The band of heavy holes of both materials have SEE with the form of a hyperboloid with one sheet. Thus the substantial difference exists between the transversal effective mass and the longitudinal effective mass. They have even the opposite signs and differ itself thereto on the modules roughly on two orders near the top of the band.

Ellipsoidal SEE characterizes the band of the light holes. The transversal effective mass exceeds the longitudinal mass on the module as for the top of this band. Consequently the SEE-ellipsoids are compressed there along the polar axis. Conversely, the situation changes itself up to the stretched out ellipsoid at approaching to the bottom of band.

Spin-orbital split band also is characterized by ellipsoidal SEE which is compressed along the polar axis. The coefficient of anisotropy does not exceed 1,8 and diminishes itself in the depth of the band. The conduct of the effective mass in addition is substantially nonlinear.

The magnitudes of the effective masses of electrons and holes nearby to the band extremes are collected into table 2. There are likewise indicated the energies of extremes as well as coefficients of anisotropy and several literary data.

The functions of the density of states for both materials and for their conductivity bands are presented by fig. 2. Both has the sole special points (M_0 type) exactly on the bottom of the located at Γ-point band. Note that density of the states is much greater for Zn_3P_2. The more or less linear dependences of the densities of states are observed inside almost entire interval of energies. The exceptions are tiny areas in proximity to extremes of the bands.

The heavy holes valence band distinguishes itself by high density of states (fig.4). Their magnitudes exceed the same for electrons on about two orders. The top of such band is a saddle point of M_2-type. The density of states has non-zero limit into this point what was shown before just for Cd_3As_2 in [17]. The additional saddle points of M_2-type were found at energies -6.7 meV and -8.7 meV for Cd_3P_2 and Zn_3P_2 respectively.

The function of the density of states has the break of the second kind at the bottom of this band. It is caused by the ultra-narrow forbidden gap between the bands of the heavy and the light holes. Nevertheless, the really low temperatures are necessary to be talking confidently about this gap as well as about the M_3-type maximum at the top of the light holes band. Otherwise both bands should be considered as virtually degenerated.

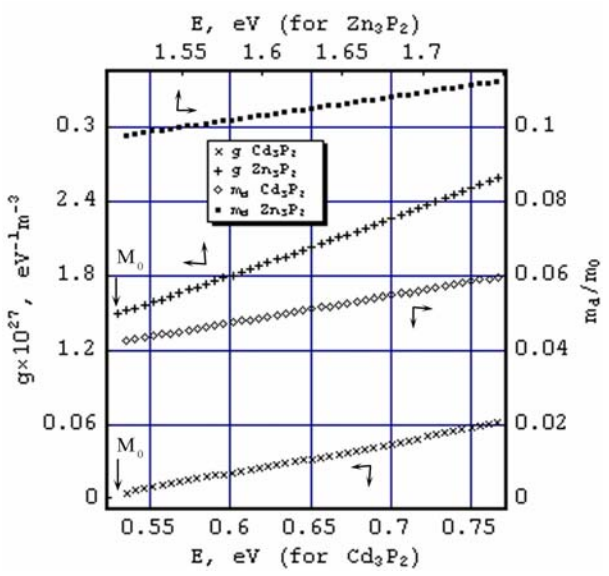

Fig. 2. Energy dependences of the effective masses of DOS and density of states for conductivity band.

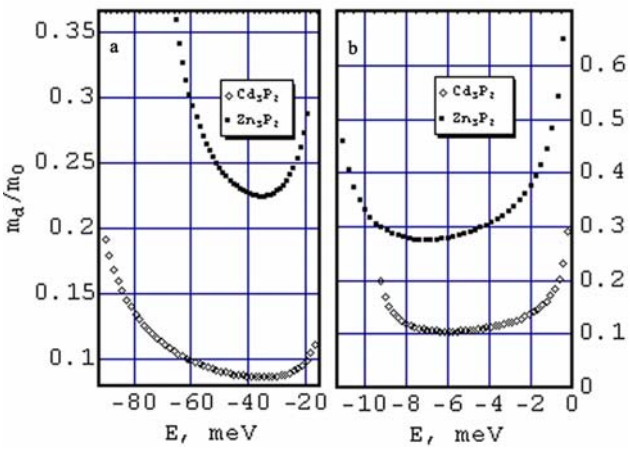

Fig. 3. Energy dependences of the effective masses of DOS for the light holes band (a) and heavy holes band (b).

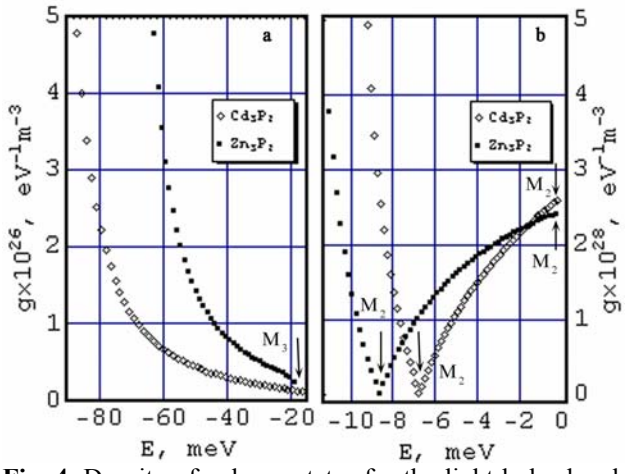

Fig. 4. Density of valence states for the light holes band (a) and heavy holes band (b).

Conclusions

1. The proposed geometrical method is simple and convenient in relation to the SEE, which are central surfaces of second order. Such state of affairs is existed either sure as for some well-known models [1] or under few additional terms as for others [2]. The method allows getting the effective masses and densities of states by simple computing procedure with high reliability.
2. Computer calculations for cadmium and zinc phosphides are presented. These results show that both conductivity bands are about isotropic, but valence bands are not definitely.
3. The entire list of the special points of the M_0, M_2 and M_3-types with their localization was found as for functions of the density of states within model of [2] for samples with the symmetry center.
4. The density of states for the top of the heavy holes band has a specific feature: non-zero limit. Similar effect was described before for the bottom of the conductivity band in Cd_3As_2 - one of few known materials having the inverted band structure like to HgTe or HgSe. These features are undoubtedly associated with the virtual degeneration of above mentioned bands with the indispensable narrow band of the heavy carriers and by one and the same reason.

Чуйко Г.П. – доктор фіз.-мат. наук, професор, завідувач кафедри загальної та прикладної фізики ХНТУ;
Степанчиков Д.М. – асистент кафедри загальної та прикладної фізики ХНТУ, аспірант.

[1] H. Kildal. Band structure of $CdGeAs_2$ near k = 0. // *Phys. Rev*., 10(12), pp.5082-5087 (1974).
[2] G.. Chuiko, N. Don, O. Dvornik, V. Ivchenko. Simple inverted band structure model for cadmium arsenide (Cd_3As_2). // *Moldavian Journ. of the Phys. Sciences*, 2(1), pp.88-94 (2003).
[3] K. Sieranski, J. Szatkowski, J. Misiewicz. Semiempirical tight-binding structure of II_3V_5 semiconductors: Cd_3P_2, Zn_3P_2, Cd_3As_2, Zn_3As_2 // *Phys. Rev*., 50(11), pp. 7331-7337 (1994).
[4] A. Kornowski, R. Eichberger, M. Giersig, et al. Preparation and photophysics of strongly luminescing Cd_3P_2 quantum dots // *Journal of physical chemistry*, 100(30), pp.12467-12472 (1996).
[5] J. Pawlikowski. Adsorption edge of Zn_3P_2. // *Phys. Rev. B*, 26(8), pp. 4711-4713 (1982).
[6] J. Cisowski. Level ordering in II_3V_2 semiconductor compounds. // *Phys. Stat. Sol*., 111(1), pp. 289 – 293 (1982).
[7] О. Маделунг. *Теория твёрдого тела*. Наука, М. 416 с. (1980).
[8] А.С. Давыдов. *Теория твёрдого тела*. Наука, М. 631 с. (1976).
[9] А.А. Абрикосов. *Основы теории металлов*. Наука, М. 520 с. (1987).
[10] G.. Chuiko, O. Dvornik, V. Ivchenko. Generalized dispersion law for 4mm symmetry ordering crystals. // *Ukranian Physical Journal*, **45**(10), pp. 1188-1192 (2000).
[11] Г.П. Чуйко, Н.М. Чуйко, О.В. Дворник. Густини станів та ефективні маси в межах узагальненої моделі Кілдал (на прикладі Cd_3P_2). // *Фізика і хімія твердого тіла*, **5**(1), с. 96-101 (2004).
[12] Г.П.Чуйко, Н.М.Чуйко. К вопросу о зонной структуре фосфида цинка и арсенида цинка в центре зоны Бриллюэна. // *ФТП*, **15**(5), с. 1208–1209 (1981).
[13] Г.П. Чуйко, О.В. Дворник. Зв'язок поміж кристалічним розщепленням валентних зон та тетрагональною деформацією гратки для сполук $A_3^{II}B_2^{V}$. // *Фізика і хімія твердого тіла*, **3**(4), с. 682-686 (2002).
[14] C. Pistorius, J. Clark, J. Geotzer, et all. High pressure phase relations and crystal structure determination for Zn_3P_2 & Cd_3P_2. // *High Press. High Temp*., **9**(4), pp. 471-482 (1977).
[15] Г.П.Чуйко. Расчет электронно-энергетического спектра арсенида кадмия, фосфида кадмия и их твердых растворов в окрестности центра зоны Бриллюэна. // *ФТП*, **14**(4), с. 629–633 (1980).
[16] J. Lin-Chung. Energy band structure of Zn_3P_2 and Cd_3P_2. // *Phys. Stat. Sol. B*., **47**(1), pp. 33-39 (1971).
[17] Г.П. Чуйко, И.А. Теплинская. Топологический переход и связанная с ним сингулярность в плотности состояний зоны проводимости как характерные свойства инверсного тетрагонального полупроводника – арсенида кадмия. // *ФТП*, **17**(6), с. 1123-1125 (1983).
[18] J.P. Jay-Garin, M.J. Aubin, L.G. Caron. Energy band structure and electron mobility of cadmium phosphide at low temperatures // *Phys. Rew. B*, **18**(10), pp. 5675-5684 (1978).
[19] M.J. Gelten, A.van Lieshout, C.van Es, F.A.P. Blom. Optical properties of Cd_3P_2 // *J. Phys.C*, **11**, pp. 227-237 (1978).

Г.П. Чуйко, Д.М. Степанчиков

Геометричний метод визначення ефективних мас та густин станів в межах узагальненої моделі Кілдал

Херсонський національний технічний університет, кафедра загальної та прикладної фізики, лабораторія теорії твердого тіла, Бериславське шосе, 24, 73008, Херсон, Україна, тел: +38(0552)326922, e-mail: step_75@mail.ru

Описано новий геометричний підхід до визначення ефективних мас та густин станів в межах узагальненої моделі Кілдал. Метод апробовано для тетрагональних фосфідів кадмію та цинку (Cd_3P_2, Zn_3P_2), що належать до просторової групи $P4_2/nmc$ (D_{4h}^{15}). Поперечні та поздовжні ефективні маси визначалися безпосередньо через півосі відповідних ізоенергетичних поверхонь. Також розраховано ефективні маси густини станів та коефіцієнти анізотропії. Показано, що запропонований геометричний підхід дозволяє надійно визначати та класифікувати сингулярні точки функції густини станів. Отримані результати показали, що зона провідності обох матеріалів є майже ізотропною, тоді як валентна зона є суттєво анізотропною. Функція густини станів для зони важких дірок має специфічну особливість: ненульову границю у вершині.